Tailoring the depth of focus for optical imaging systems using a Fourier transform approach

Jeffrey A. Davis and C. Stewart Tuvey

San Diego State University, Department of Physics, San Diego, California 92182, USA

Octavio López-Coronado, Juan Campos, and Maria J. Yzuel

Departamento de Fisica, Universidad Autonoma de Barcelona, 08193 Bellaterra, Spain

Claudio Iemmi

Departamento de Fisica, Facultad de Ciencias Exactas y Naturales, Universidad de Buenos Aires, (1428) Buenos Aires, Argentina

Received November 22, 2006; revised December 14, 2006; accepted December 14, 2006; posted January 19, 2007 (Doc. ID 77345); published March 5, 2007

We show how to tailor the depth of focus for an optical system using pupil functions obtained from a Fourier transform approach. These complex amplitude and phase pupil functions are encoded onto a single liquid-crystal spatial light modulator. Experimental results show excellent agreement with theory and indicate the power of this approach. © 2007 Optical Society of America

OCIS codes: 110.0110, 110.2990, 090.1970, 230.6120, 230.3720.

The transverse and axial imaging capabilities of optical systems can be improved by using specially designed pupil functions with such design goals as superresolution and extended depth of focus. An extremely powerful approach for studying axial imaging was first introduced by McCutchen,[1] where the axial intensity response near the focus is given by the one-dimensional Fourier transform of the radially symmetric pupil function expressed in r^2 coordinates. The advantage of the Fourier transform formalism is that it gives some intuitive guidance for the design of new pupil functions. Although some theoretical results have been obtained with this formalism,[2–4] much of the theoretical effort has gone into numerical simulations in which various design parameters are optimized.[5]

Experimental results are surprisingly limited because of the difficulty in constructing these pupil functions. Binary phase diffractive optical elements,[5,6] consisting of annular rings, have been fabricated and produced good results. Amplitude pupil functions, consisting of polynomial series, have been encoded[7,8] onto liquid-crystal spatial light modulators (LCSLMs). More recently, combined amplitude and phase pupil functions were reported[9] in an attempt to increase the information encoded on the pupil function.

In this Letter we directly utilize the Fourier transform approach to generate pupil functions that create desired depth of focus distributions. Several goals are pupil functions that create a long uniform (rectangular) depth of focus, a triangular depth of focus where the intensity increases to a maximum at the focal point and then decreases, and finally a dual focus dependence consisting of two separated rectangular regions. These complex (amplitude and phase) pupil functions are then encoded onto a single LCSLM. In practice, we must use iterative techniques to overcome the limitations imposed by the limited number of pixels on the LCSLM. Experimental results are extremely good.

Next we outline the theory of these pupil functions. We assume an axially symmetric lens function $t(r)$ written as the product of a converging lens with focal length f and a complex pupil function $p(r)$ as $t(f,r) = p(r)\exp(-ikr^2/2f)$. Using Fresnel diffraction and assuming axial symmetry, the scalar electric field at the origin of the viewing plane ($x_2 = y_2 = 0$) located a distance $z \approx f$ from the input plane is given by

$$E(x_2 = 0, y_2 = 0, z) = \frac{i}{\lambda z}\int_0^a p(r)\exp\left(\frac{-ikr^2}{2f}\right)\exp\left(\frac{ikr^2}{2z}\right)2\pi r\mathrm{d}r. \quad (1)$$

Here a is the radius of the pupil function. We ignore constant phase terms and $k = 2\pi/\lambda$, where λ is the wavelength. We define normalized axial coordinates $u = a^2/2\lambda z$ and $u_0 = a^2/2\lambda f$. We approximate the leading $1/z$ term by $1/f$ (Ref. 10) to simplify the equation. In practice, this leads to an error of less than 4% that cannot be seen in the experimental results. Next we define the variable $s = r^2/a^2 - 0.5$ that varies from -0.5 to $+0.5$. The integral is now symmetric with respect to the new origin and can be rewritten as a Fourier transform integral by extending the limits of integration to infinity as

$$E'(u) \approx \int_{-\infty}^{\infty} q(s)\exp(-i2\pi u_0 s)\exp(i2\pi u s)\mathrm{d}s. \quad (2)$$

Here the pupil function is rewritten in terms of the new variables as $q(s)$.

Because the Fourier transform of the product of two functions is the convolution of their Fourier transforms, we rewrite the integral of Eq. (2) as

$$E'(u) \approx \delta(u - u_0) \otimes Q(u). \quad (3)$$

0146-9592/07/070844-3/$15.00

Consequently the axial electric field $E'(u)$ is proportional to the Fourier transform $Q(u)$ of the pupil function $q(s)$ expressed in s coordinates. For a rectangular pupil function, the electric field is a sinc function in the u direction centered at the focal point of the lens. As the pupil aperture a decreases, the focus broadens along the z axis. We can relate the u and z dimensions by using $u-u_0 \cong a^2(z-f)/(2\lambda f^2)$.

The initial results using the fast Fourier transform (FFT) were good, but there were problems (such as the Gibbs overshoot in the rectangle response functions) because the pupil function is spatially limited by the size of our LCSLM. Consequently we used an iterative design procedure[11,12] as outlined in Fig. 1 to improve the results. Figure 1(a) shows the desired output axial response function $E'(u)$ (a rectangle, for example). We use discrete Fourier transforms having $N_1=512$ points (or samples) and define the axial response function over a limited region of m points (from u_1 to u_2). By performing the Fourier transform, we obtain the complex transmission of the pupil $q(s)$ as shown in Fig. 1(b). We cannot use this entire distribution because of the finite size of the LCSLM. Consequently we truncate the pupil function to $N_2=256$ points, where the regions outside the pupil (s_1–s_2) are made equal to zero as shown in Fig. 1(c). By inverse Fourier transformation we obtain the axial distribution $Q(u)$ in Fig. 1(d), and we find that it does not coincide with the desired one because of the restrictions mentioned above.

To improve the results, we impose additional restrictions. In the region (u_1–u_2) we restore the originally designed magnitude of the axial distribution. The axial phase distribution is used as a degree of freedom. Outside this region the magnitude is truncated if it exceeds a given percent (5% for this example) of the maximum magnitude in the region (u_1–u_2). Then a new axial distribution is obtained. We continued the process until the mean square error was 0.01 (in the case of the double rectangle, we were limited to a value of 0.1). Typically this required about 1000 iterations. However, because of the efficiency of the FFT algorithm, this typically required a few seconds.

After this procedure is completed, the pupil function $q(s)$ must be rescaled to the radial coordinates as $p(r)$. This rescaling spreads the central radial portion and compresses the outer parts. This compression can create problems because fast oscillations in the pupil function are difficult to encode onto the limited pixel structure of the LCSLM.

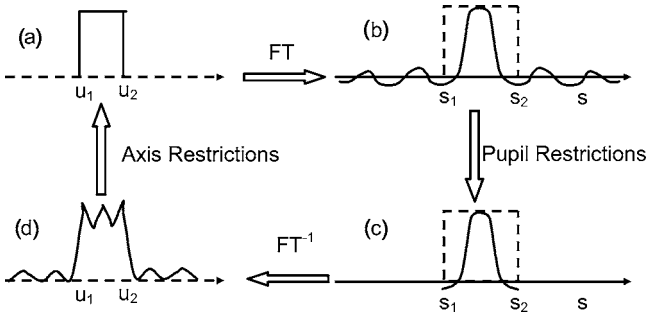

Fig. 1. Iterative filter design.

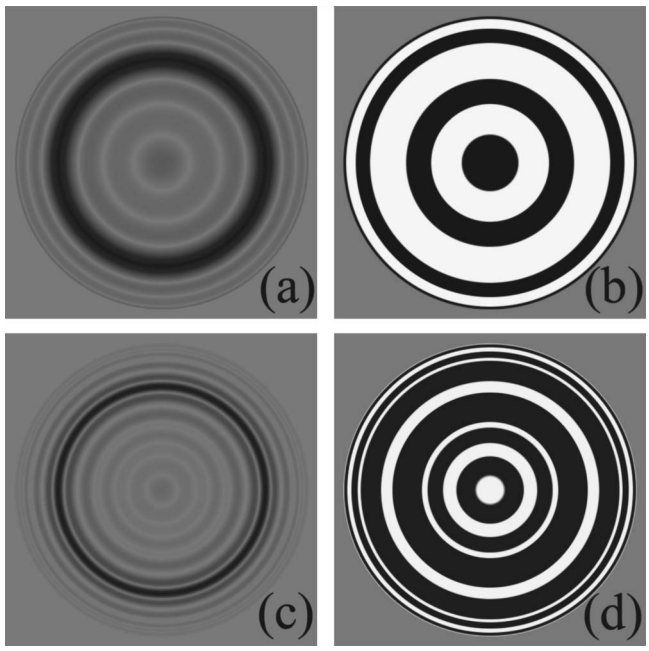

Fig. 2. Amplitude and phase distributions for functions that give an axial response: (a), (b) rectangle having 9 points; (c), (d) two 9-point rectangles separated by 21 points.

To demonstrate this approach, we designed several pupil functions. Figure 2 shows the amplitude and phase for pupil functions $p(r)$ that yield a rectangular [Figs. 2(a) and 2(b)] and two-separated-rectangle [Figs. 2(c) and 2(d)] axial response functions. Using the simple Fourier transform relation between the widths of the rectangle and sinc functions, the axial distance in z coordinates is related to the number of samples in the rectangle function as

$$L = (2m\lambda f^2 N_2)/(N_1 a^2). \tag{4}$$

The experimental setup is similar to that reported earlier.[8] Linearly polarized light from an argon laser is spatially filtered, expanded, and collimated. The pupil functions are encoded onto a parallel-aligned nematic LCSLM manufactured by Seiko Epson with 640×480 pixels having dimensions of $42\,\mu$m on a 1.3 in. display.[13] Each pixel acts as an electrically controllable phase plate where the total phase shift exceeds 2π rad as a function of gray level at the argon laser wavelength of 514.5 nm. The light is focused by a 38.1 cm focal length Space Optics Research Labs lens. Because the focal spot size from the lens is extremely small, we magnify it with a $20\times$ microscope objective lens. We fix the distance between the microscope objective and the detector, and by shifting the assembly (objective plus CCD camera) along the axis, we measure the peak intensity in the transverse plane at different axial distances.

Our LCSLM is easily capable of encoding the phase information. Amplitude information is then encoded onto this phase-only medium by spatially modulating the phase pattern with the amplitude portion of the pupil function.[14] As the phase depth increases, the in-

tensity diffracted into the first order increases, while the zero-order intensity decreases. We first multiply the pupil function with a linear phase grating having a period $d=6$ pixels. Now the total phase is the sum of the pupil phase term with the grating phase. Finally, we multiply this phase pattern by the magnitude of the pupil function so that the total phase is given by $\exp\{i|p(r)|[\phi(r)+2\pi x/d]\}$. Here the phase is in the range $[-\pi,\pi]$, and the amplitude is defined in the range $[0\leq|p(r)|\leq 1]$.

Experimental results are shown in Fig. 3. Figure 3(a) shows the axial intensity distribution for a clear pupil having a radius of 10 mm. The depth of focus measured between the minima of the sinc-squared intensity distribution is 2.8 mm, in excellent agreement with theory. Figures 3(b)–3(d) show the axial distributions for a series of pupil functions having initial lengths of $m=9$, 21, 41 points in the Fourier transform program. The depth of focus now increases up to 30 mm. Next we designed a pupil function to produce an electric field that varied axially as $\sqrt{z}$ and a triangular intensity distribution with a length equivalent to 41 points. Figure 3(e) shows the experimental triangular intensity distribution. Finally, Fig. 3(f) shows the output where we programmed two rectangle functions having widths of 15 points separated by 25 points. Experimental error is about 10%, caused by fluctuations in the laser intensity and vibrations.

There are several limitations with this approach. The transmission efficiency of these pupil functions is reduced because the complex pupils absorb some of the incident light. There are also difficulties in implementing the pupil function designs. As the length of the distribution in the u domain decreases, the information available for the pupil decreases—we have fewer sidelobes to encode. This causes low pass filtering of the output response. On the other hand, as the u domain length increases, the number of sidelobes increases. Now it is much more difficult to encode the rapidly varying pupil function (particularly when it is rewritten into the r domain) with the limited number of pixels.

Nevertheless, the experimental results are excellent and agree well with the predictions of Eq. (4). For the case of Fig. 3(c), we have extended the depth of focus by a factor of over 20 compared with the original open pupil. This approach shows the power of the Fourier transform formalism and shows that these kinds of complicated pupil functions can be easily constructed with a single LCSLM to obtain a desired axial response of an optical system.

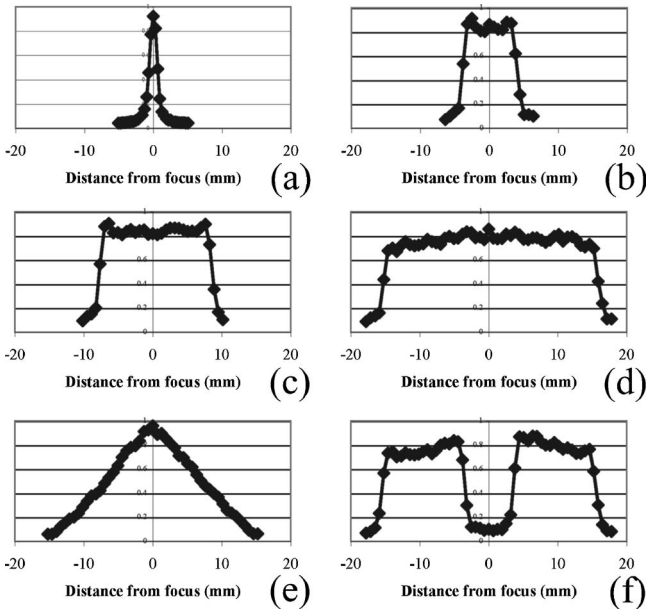

Fig. 3. Axial intensity response (arbitrary units) obtained for (a) uniform pupil, (b) 9 point rectangle, (c) 21 point rectangle, (d) 41 point rectangle, (e) triangle, (f) two 15 point rectangles separated by 25 points.

We acknowledge financial support from the Spanish Ministerio de Ciencia y Tecnología (grant FIS2006-13037-C02-01). C. Iemmi gratefully acknowledges the support of the Universidad de Buenos Aires and Consejo Nacional de Investigaciones Científicas y Técnicas (Argentina). We thank Tomio Sonehara of Seiko Epson Corporation for the use of the LCD and Don Cottrell for his computer program. J. A. Davis's e-mail address is jdavis@sciences.sdsu.edu.

References

1. C. W. McCutchen, J. Opt. Soc. Am. **54**, 240 (1964).
2. J. Ojeda-Castañeda, L. R. Berriel-Valdos, and E. Montes, Opt. Lett. **10**, 520 (1985).
3. J. Ojeda-Castañeda, E. Tepichin, and A. Diaz, Appl. Opt. **28**, 2666 (1989).
4. J. Ojeda-Castañeda and L. R. Berriel-Valdos, Appl. Opt. **29**, 994 (1990).
5. J. Jia, C. Zhou, Z. Sun, and L. Liu, Appl. Opt. **43**, 2112 (2004), and references therein.
6. H. Liu, Y. Yan, and G. Jin, Appl. Opt. **40**, 2316 (2001).
7. J. A. Davis, J. C. Escalera, J. Campos, A. Marquez, M. J. Yzuel, and C. Iemmi, Opt. Lett. **24**, 628 (1999).
8. A. Marquez, C. Iemmi, J. C. Escalera, J. Campos, S. Ledesma, J. A. Davis, and M. J. Yzuel, Appl. Opt. **40**, 2316 (2001).
9. P. N. Gundu and E. Hack, Opt. Express **13**, 2835 (2005).
10. M. V. Klein, *Optics* (Wiley, 1970), Chap. 9.3.
11. J. Rosen and J. Shamir, Opt. Lett. **16**, 752 (1991).
12. D. C. Youla and H. Webb, IEEE Trans. Med. Imaging **MI-1**, 81 (1982).
13. J. A. Davis, P. Tsai, D. M. Cottrell, T. Sonehara, and J. Amako, Opt. Eng. **38**, 105l (1999).
14. J. A. Davis, D. M. Cottrell, J. Campos, M. J. Yzuel, and I. Moreno, Appl. Opt. **38**, 5004 (1999).